Electrotunable Friction with Ionic Liquid Lubricants

Fernando Bresme[1], Alexei A. Kornyshev[1], Susan Perkin[2] and Michael Urbakh[3]

[1] Department of Chemistry, Molecular Sciences Research Hub, Imperial College London, W12 0BZ London, U.K

[2]Physical and Theoretical Chemistry Laboratory, Department of Chemistry, University of Oxford, Oxford, UK

[3]Department of Physical Chemistry, School of Chemistry, The Raymond and Beverly Sackler Faculty of Exact Sciences, and The Sackler Center for Computational Molecular and Materials Science, Tel Aviv University, Tel Aviv 6997801, Israel

Abstract

Room temperature ionic liquids and their mixtures with organic solvents as lubricants open a route to control lubricity at the nanoscale via electrical polarization of the sliding surfaces. Electro-nanotribology is an emerging field that has a potential to realize in situ control of friction, i.e. turning the friction on and off on demand. However, fulfilling its promise needs more research. Here we provide an overview of this emerging research area, from its birth to the current state, reviewing the main achievements in nonequilibrium molecular dynamics simulations and experiments using atomic force microscopes and surface force apparatus. We also present a discussion of the challenges that need to be solved for the future applications of electrotunable friction.

Tribology, the science of friction, wear, and lubrication, is of fundamental importance for many branches of pure and applied science. A considerable part of the world's energy consumption (~23%) originates from tribological contacts, namely, energy losses in friction and manufacturing of worn parts[1]. While the term *tribology* emerged in the 1970's [2], the history of friction science is much older. Its first laws were formulated by Amontons[3] at the end of the 17th century, but some of them were known to da Vinci[4]. In the 18th century, Coulomb performed pioneering studies of static and kinetic friction,[5] and Cavendish and Hutchett addressed friction-induced wear. In 1950, Bowden and Tabor came up with the first approach to understanding physical mechanisms of friction and wear.[6] They introduced the asperity contact theory, describing friction as resistance to motion arising from adhesion and irreversible deformation of the interfaces.

Traditionally, tribology was a discipline of contact mechanics. However, in the 21st century, it has become an interdisciplinary part of material science – at the interface of solid state, molecular, and nonlinear physics, statistical mechanics, physical chemistry, fluid and solid mechanics, nanoscience, and nanoengineering. The past two decades uncovered new challenges and opportunities for tribology, following the fabrication of micro and nano-electromechanical systems (MEMS and NEMS), which have revolutionized many technologies by exploiting new physics emerging at small length scales. Generally, the high surface-to-volume ratio in these miniature devices results in severe friction and wear, limiting their use and lifespan. *Nanotribology*[7,8,9] - a field of studying friction at the nanometer scale, provides a bottom-up, atomistic approach to designing new low-friction materials with unique characteristics[10,11,12,13]. In parallel with this, the importance of nanoscale lubrication to macroscopic systems is becoming widely acknowledged. Even for large surface-area contacts, the lubrication and friction are, in most cases, determined by the properties of 'nanofilms' just a few molecular layers thick. Understanding and controlling the dissipation of energy across such films are the fundamental tasks of nanotribology.

Substantial progress in understanding the properties of nano-films under different load, shear and temperature conditions was achieved recently, and new factors affecting friction were unraveled. [7,8,9] Obviously, friction can be modified by changing the properties of the lubricant or shearing surfaces, but a new direction for nanotribology lies in approaches to switch and control surface interactions at the molecular level, tuning friction reversibly in real time, using non-invasive mechanisms. Such control over friction would be instrumental for automotive, aerospace, electronic, and microrobotics industries; in macroscopic bearings – for instance in lightweight vehicles, lifts or more generally rotating shafts, which can be deployed also in energy recovery applications and medicine (prosthetics, drug release).

Previous approaches to the dynamic control of adhesion and friction involved mechanical modulations of normal and lateral forces[14,15] or light irradiation[16]. In the case of electronically conducting sliding contacts a more robust, natural, and readily implementable approach is applying an electric potential to control the lubricating properties of nanofilms[17]. Examples of electromagnetic tuning of friction in nano-, micro- and macroscale systems demonstrating the variety and versatility of these approaches are overviewed in Ref.18. Variations of the static electric field can significantly modify the composition, structure, and dynamics of the lubricating film. This can be done by less than 1V variation of applied voltage for an electrolytic solution or ionic liquid lubricant. The potentials of such sliding surfaces can be independently varied relative to a reference electrode in the bulk, enabling their symmetric or asymmetric polarization. This approach has been successfully used in Atomic Force Microscopy (AFM) measurements[19,20,21,22,23] (see Fig.1). The Surface Force Apparatus (SFA) provides another route to investigate nanofilms[12,24,25]; real-time control of the surface charges (potential) in SFA has recently been achieved[26 27,28,29,30]. This was made possible by creating ultra-flat conducting surfaces (e.g. covering mica surfaces with graphene)[28,28] , or replacing mica surfaces with molecularly smooth gold electrodes[31] .

Advantages of electrolytic lubricants for electrical control of friction are obvious. The electrolyte ions are strongly influenced by the electrostatic fields from the surfaces, and the structure and dynamics of the lubricant can therefore be controlled externally. In that respect, Room Temperature Ionic Liquids (RTILs) – complex molten salts with melting points below 100^{o}C, are most attractive, due to their unique thermophysical properties (low vapor pressure, high thermal stability, wide electrochemical stability window) and virtually unlimited variety of compositions[32,33,34]. Ionic liquids consist of organic salts or mixtures of organic components, with common salts including, e.g. alkylammonium, alkylpyridinium or alkyimidazolium cations, and tetrafluoroborate, hexafluorophosphate or bis(trifluoromethylsulfonyl)imide anions. RTILs are hygroscopic and absorb water from humid air. The hydrophilicity is determined to a large extent by the anion. RTILs can undergo tribo-chemical reactions, and the ions can be oxidized (e.g. phosphonium to phosphate) during the measurements[35]. It is expected that this will lead to protecting layers[36] similar to those observed with conventional lubricants, however the interplay between Electrotuneable Friction (EF) and triboelectrochemistry has yet to be systematically studied.

RTILs interact strongly with solid surfaces, particularly when the latter are charged, providing wear-protective films sustaining higher normal loads than those of existing molecular lubricants[11,37]. The interaction of RTILs with confining surfaces leads to fascinating structural and dynamic features such as layering, overscreening and crowding[33,34,38], discrete multi-valued friction depending on the number of confined ionic layers ("quantized friction")[39], nanoscale capillary freezing[40], and EF[20,21].

For the same RTIL lubricant, under given conditions (normal load, shearing velocity and temperature) the friction can be reversibly tuned via electrical polarization of the surfaces. AFM experiments with RTILs confined between a silica tip and graphite surface[21,41] demonstrated that super-low friction (superlubricity) can be ‘‘switched’’ on and off, by polarizing the surface.

The electric field built up across the RTIL nanofilm induces alternating positive (cation) and negative (anion) ionic layers[33,34], with an interlayer separation that corresponds to the ion pair size[25,39,42,43,44,45]. Switching the field can modify the composition and/or arrangement of these ions and therefore the overall friction characteristics of the film – see Box 1. Voltage-control through rearrangement of ions between chargeable surfaces has been widely used in polymer-electrolyte based electroactuators[46] or electrowetting[47]. In EF, we deal with ‘electroactuation’ on the molecular level using ‘electroactive lubricants’, where depending on how one polarizes the electrodes, both the nanofilm thickness, the distribution of ions (including the ratio of anions and cations), or even the phase behavior and relaxation timescale of the film can be changed.

Despite significant advances in experimental and theoretical studies of EF with RTIL-lubricants, many aspects remain to be better understood:

i) What are the microscopic mechanisms behind the frictional phenomena observed in RTIL nanofilms?

ii) Which experimental conditions lead to optimum EF and significant reversible variation of friction with voltage?

iii) What materials and liquids would be best suited for this?

iv) Can EF help to reach superlubricity in otherwise frictional contacts?

v) What is the mechanism of friction in mixtures of RTILs with organic solvents, and what is the minimal ionic concentration required to ensure EF in these mixtures?

Unlike previous reviews on lubrication with RTILs[11,48], here we focus on discussion of key challenges on the way to robust EF.

Experimental configurations for voltage-control of friction

Interrogating EF mechanisms experimentally requires measurement of the i) film thickness and ii) normal force acting between two surfaces with a liquid film in between, iii) electrostatic polarization of surfaces applied *in situ,* and iv) simultaneous sliding motion and detection of the lateral force. Techniques well suited to these specifications and allowing for molecular-level resolution are AFM[20,21] and SFA[28,49,50,51] (Fig.1). Importantly, it has been demonstrated that only relatively modest electrical bias (~1V) causes a substantial reorganization of the electrical double layer, with the strongest influence felt by the ion layers closest to the electrode surface[52]. The applied voltage induces a charge on the surface, which in turn alters the near-surface liquid structure in striking ways. Indeed, at neutral surfaces, unless the ions are preferentially adsorbed, cations and anions form mixed layers. At charged surfaces, at least for not too large voltages, they form layers of alternating net charge [33,34] (see Figs. 1 and 2a,b). Formation of such layers affects the mechanisms of shear dissipation and friction forces across the film. For example, Sweeney et al.[20] reported the strong confinement of cations when one surface was negatively polarised, leading to a friction coefficient reduced by a factor of three compared to positively polarised surfaces. Conversely, Li et al.[21] showed that applying +1.5V *vs* Pt reference led to positive charging of the HOPG surface and subsequent coating by an anion layer leading to a reduction in friction at the contact.

Box 1 | Charging configurations.

The experiments on EF can be summarized according to their various configurations; see Box 1 figure below. Until now, most experiments have involved setting up a potential difference between one or both surfaces relative to an electrode away from the contact in the bulk of the lubricant fluid, as shown in panel A of Box 1 figure for symmetric surface polarization. In general, such polarization influences friction in two related ways: first RTILs in the confined nanofilm respond to the surface charging by expelling co-ions and/or attracting counterions to retain local electroneutrality (see switching of film composition in the Box 1 figure, mechanism i)). This change in the anion/cation ratio, effectively the *composition* of the film, can modify the friction coefficient, for example by accumulating a monolayer of cations with flexible alkyl chains[20]. Secondly, charging of the surfaces modifies the normal force (pressure) between the surfaces that can drive them together or apart, thus modifying the *thickness* of the film[28]. The 'symmetry-breaking' effects in compositions and forces arise from different characteristics of the cations and anions (shape and their intra-molecular charge distributions), leading to modified friction when the lubricant film is rich in cations or in anions.

One challenge faced when transferring this concept to devices is locating a suitable counter electrode appropriately close to the moving contact. Addressing this, it has been proposed that a potential difference is instead applied between the two shearing surfaces themselves, leading to asymmetric polarization as shown in Box 1 figure, panel B. Here, the two surfaces separated by the lubricating film are oppositely charged, leading to different prospects for tuning the lubrication of the contact. In this case, on average, there will be no excess charge in the film, so that the cation/anion ratio there will remain unchanged. However, both the pressure between the surfaces and the dynamics in the liquid film will be affected by the resulting electric field between the surfaces, creating alternative routes to tuning the lubricity of the film. Various lubrication switching scenarios are possible, dependent on the AC timescale relative to relaxation timescales in the electrolyte film; low AC frequencies will allow for ion reorganization (mechanism ii)) whereas high AC frequencies lead to unscreened electric fields between the surfaces (mechanism iii)) which can be switched on and off to control friction. Until now, only a couple of experiments used a setup of this sort: one experiment involving a confined polyelectrolytic film[49] demonstrated an 80% reduction in friction using an alternating electric field. This exciting result, combined with emerging evidence that AC electric fields cause very large repulsive forces across ionic films, signals strong prospects for AC-controlled friction[30,53,54]; to date it remains to be demonstrated if EF with pure RTILs can be realized in this way. AC signal with frequencies faster than the timescale of electrical double layer charging, to avoid electrical breakdown and to reach more complex effects , are clearly possible and are envisaged as a powerful tool for tuning surface interactions and friction[30, 53, 54].

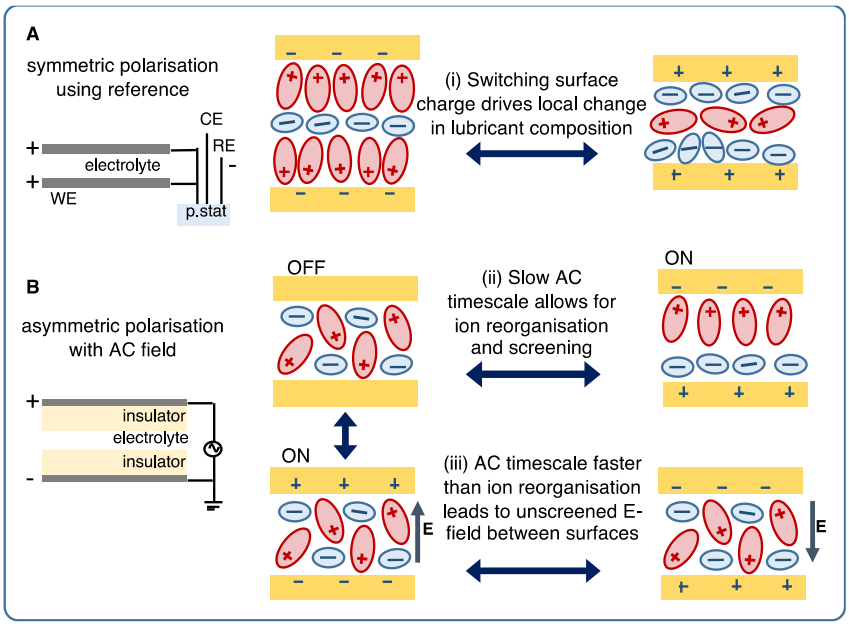

The charging of confining plates leads to i) formation of ionic layers of alternating charge accompanied by overscreening[43] at small and moderate surface charges (< 30 μC/cm2); ii) full charge compensation of the surface for charge densities similar to those found in mica (-32 μC/cm^2); and iii)– crowding of counterions at higher charge densities. Overscreening is defined as the emergence of a net charge in the first layer adjacent to the surface, opposite in sign to the charge of the surface, but having the absolute value higher than the latter (see middle panel in Fig.3a). The next layer has a charge opposite in sign to the sum of the mentioned two charges, but again of the larger absolute value. This results in decaying charge density oscillations extended over several layers before reaching electroneutrality. With further increase of the surface charge, the system will reach the point when there is no more room in the first layer to accommodate enough counterions to overscreen the charge of the surface. The next layer may still overscreen the net charge of the surface and first layer. With charge of the surface increasing, the second layer may then also get saturated with counterions, and so on, which leads to the so called counterion crowding regime[38]. The latter would happen at very large charges, at the edge of experimental accessibility. The effects of overscreening and, to a less extent, crowding, will be manifested in nanoconfinement, but not literally as in semi-infinite systems, as they will be affected by the interplay between the size of the ions and the width of the nanogap accommodating them. Experimental studies using X-ray reflectivity[70], neutron reflectivity[55], AFM[41], sum-frequency vibrational spectroscopy[56], are broadly consistent with an enrichment of counterions at charged surfaces, as well as with the microscopic images provided by molecular simulations.

< End of Box 1 >

In bringing such experimental proof-of-concept towards practical implementation, it is necessary to inspect the role of water, surface roughness, and other parameters not present in the model experiments. Studies of friction forces across RTIL films with control over added water content show diverging outcomes, indicating that several competing mechanisms may be simultaneously in charge, such as the altered location of the slip plane and enhancement of surface ordering[57,58,59,60].

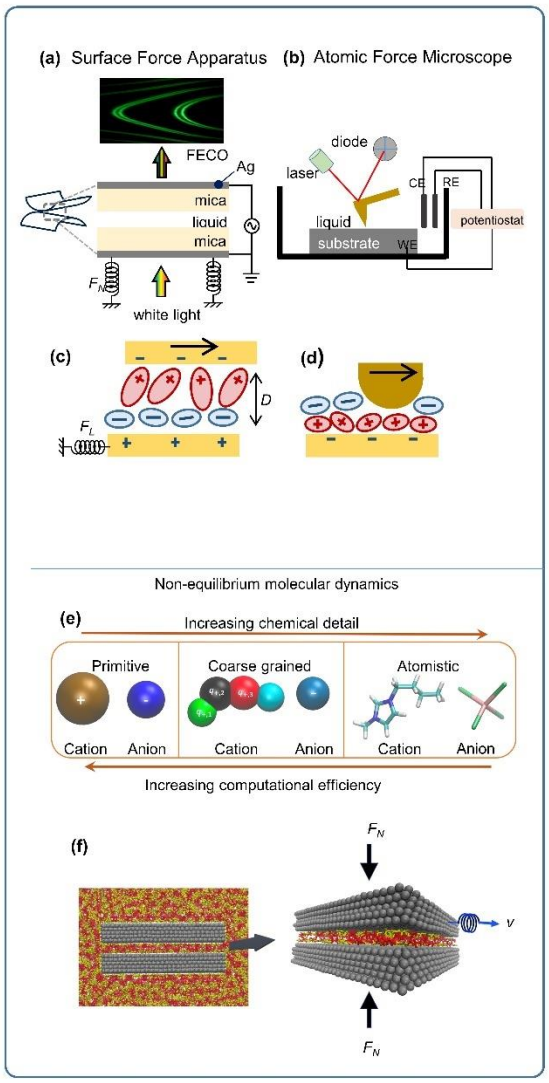

Fig. 1. Experimental and simulation approaches to study electrotunable friction with lubricating nanoscale RTIL films. (**a**, **b**) Schematics of SFA and AFM setups for voltage control of friction. SFA uses two identical macroscopic substrates in crossed-cylinder geometry (left) with large (~1 cm) radius of curvature, much greater than the molecular scale. Interferometry is used to determine liquid film thickness and forces via spring deflections (shown top is a typical spectrum showing the fringes of equal chromatic order, FECO). The surfaces typically consist of silver (Ag) layers behind mica sheets; Ag acts as both mirror and electrode. Mica acts as a dielectric spacer. Surfaces can be polarized symmetrically (not shown) or asymmetrically (as shown). AFM uses a sharp (~ 5 nm) tip interacting with a planar substrate; forces are measured using a laser to measure cantilever normal and torsional deflections. Until now most EF measurements with AFM involved voltage control of a single planar electrode relative to a reference in the bulk fluid, with the tip electrically isolated. However, both SFA and AFM can incorporate various electrical and electrochemical arrangements; see Box 1 for further possibilities. (**c**, **d**) Sketch of RTIL structure confined between charged mica surfaces in SFA configuration (**c**), and between a tip and electrode in AFM setup (**d**). (**e**, **f**) Schematics and relevant quantities of Non-equilibrium Molecular Dynamics (NEMD) Simulations of EF: (**e**) Three types of force-fields employed to simulate RTILs in NEMD: primitive, coarse-grained, and atomistic (see Box 2). (**f**) Simulation set up employed for NEMD of EF. The ionic liquid is confined between solid slabs at nanometer separation (see right panel), and under a normal load F_N, acting on both slabs. One of the slabs is pulled through a spring at constant sliding velocity, v.

Microscopic insights into Electrotunable Friction

The theoretical methods available to investigate friction in nanoscale liquid films range from ‘‘minimalistic’’ models, such as the Prandtl-Tomlinson and Frenkel-Kontorova models, to computer simulation. The minimalistic models provide qualitative insight into stick-slip motion, the transition to sliding or superlubricity [9]. However, a deeper understanding of friction and its dependence on the molecular structure of lubricating films, normal load, temperature, or surface charge density, requires molecular-level approaches. The approaches to investigate EF in RTILs using molecular simulations (MS) are discussed in Box 2.

Box 2 | Modelling EF with ionic liquid lubricants

MS are widely used to investigate materials and fluids at experimental conditions relevant to friction (temperature, load, shear rate, inter-surface distance, degree of surface roughness or heterogeneous composition)[9]. Non-equilibrium computer simulations[61] allow to interrogate the response of the films under nanoconfinement, by integrating the trajectories of atoms interacting through intermolecular forces. The MSs of lubricated friction often mimic the set-up used in AFM or SFA experiments (see Fig. 1f). The choice of the interaction force fields between atoms is the first step to simulate RTILs in nanoconfinement. The ions can be modelled at different levels: Primitive models (see Fig. 1e) that provide the simplest forcefields, capturing size asymmetry, were employed in the first simulations of EF[62]. Coarse-Grained (CG) models incorporate some chemical specificity by mapping groups of atoms into a single bead and distributing the net charge amongst different pseudo-atoms (see Fig. 1e)[63,64,65,66]. Atomistic models[67,68] target the full structural complexity of the ions (see Fig. 1e), providing higher level of detail in computer simulations; an example of $BMIM^+$ BF_4^- is shown in the right panel of Fig 1e. CG models are computationally efficient, which is advantageous as RTILs feature high viscosities (up to ~30-100 times higher than water), and low diffusion coefficients (two orders of magnitude lower than water, $\sim 10^{-11}$ m^2/s). CG models were used to study friction as a function of the RTIL composition, surface charge, normal load and pulling speed. MSs can also be used to simulate surfaces commonly employed in friction experiments (mica[25,39], silica[69] and metallic surfaces[42,20,70,71]).

In MS of EF the confined RTIL and the solid slabs are immersed in a reservoir of the bulk ionic liquid. The ions can enter or leave the confined region in response to changes in load or sliding velocity (see Figure 1f). Hence, the number of ions in the confined region can change during the simulation, subject to sliding and the swelling of the film. In the stationary regime, the chemical potentials of the RTIL in the confined and bulk regions are the same. Different surface charge

densities can be modelled by charging uniformly the layer of atoms in the slabs that are in direct contact with the confined RTIL.

The surface charge can be modelled using the fixed charge method (FCM), in which the charge on each surface atom is constant throughout the simulation[62,], or *the constant potential method* (CPM) [72,73], where the charge distribution on the surfaces is adjusted self-consistently, subject to the electrical capacitance of the frictional contact. Differences between the two methods might be expected for metallic surfaces, as the electrode potential, not the charge, is kept constant. Simulations of RTILs nanofilms (1-10 nm thick) showed, however, that the differences between the FCM and CPM become significant only at very high voltages $\geq$4V [72,74], which are close to or above the limit that most of the RTILs at electrodes can withstand without oxidation or reduction of the ions. The similarity between FCM and CPM results can be rationalized by considering the strong screening of image charges by the first layer of counterions at the metallic surface.

Standard MS of EF is performed with length scales like those featuring in sliding contacts (~nm) and sliding speeds of the order of 1-10 m/s, which approach the speeds of interest in practical applications. These speeds are significantly higher than those occurring in nanoscale friction experiments with AFMs and SFA (10^{-3}-10 $\mu m/s$). To match experimental conditions, accelerated MSs has been employed to study stick-slip friction in nanoscale solid-solid contacts[75] for sliding speed as low as 25 $\mu m/s$, revealing the importance of thermal activation processes in atomic stick-slip dynamics. These MS reported a weak, logarithmic dependence of friction on the sliding speed, which is usually observed in the stick-slip regime and allowed a reliable interpretation of energetic aspects (sliding potential energy barriers) of AFM and SFA.

MS methods can also be extended to include chemical reactivity between the lubricant and the confining surface and tackle tribochemistry problems and corrosion, which have become increasingly popular in the last years. Such simulations rely on quantum approaches to model formation and breaking of chemical bonds (Density Functional Theory, Quantum Mechanics/Molecular Mechanics, Reactive Force-fields)[76]. They complement surface chemistry techniques such as Scanning Electron Microscopy, STEM, or XPS[70] by providing a microscopic view of tribofilms 'in situ'.

< End of box 2 >

The layering and charge structure of RTIL nanofilms confined between mineral or metallic surfaces has been examined recently using experiments and MS. The simulated distance-pressure isotherms feature discontinuous jumps of the order of an ion diameter or ion-pair size, 0.5-1 nm (see Fig. 2b)[52,66,77] . The jumps emerge from the squeezing out of molecular layers upon compression ("odd" or "even" number, when the nanofilms are confined between like or unlike charged surfaces, respectively)[62,72,78,42,64,66]. Bi-layer ejection is consistent with the overall electroneutrality condition observed in SFA experiments, while single layer ejection has also been reported in AFM[23] and explained by MS[79] (Fig.2a). MS-studies showed that nanofilms withstand very high pressures (0.1-1 GPa), demonstrating an excellent performance of RTIL lubricants protecting surfaces from wear.

Lateral (in-plane) ordering and crystallisation (see Fig.2c) has been demonstrated in MS using CG and atomistic models[62,64,78,80,81,82,83]. This behavior is consistent with experiments using small ions (EMIM NTF_2) confined between a magnetic AFM tip and a gold (100) surface[84], which provided evidence for epitaxy induced crystallization in the confined liquid. Interestingly, the in-plane ordering in the layers adjacent to the substrate and in the interior of the film can proceed even without strong epitaxy and affect the slippage plane position and friction. Film crystallization with larger cations (e.g. those containing long aliphatic chains in imidazolium salts) is more costly, entropically, and nanofilms form hydrophobic / hydrophilic disordered domains[70,85,86,88].

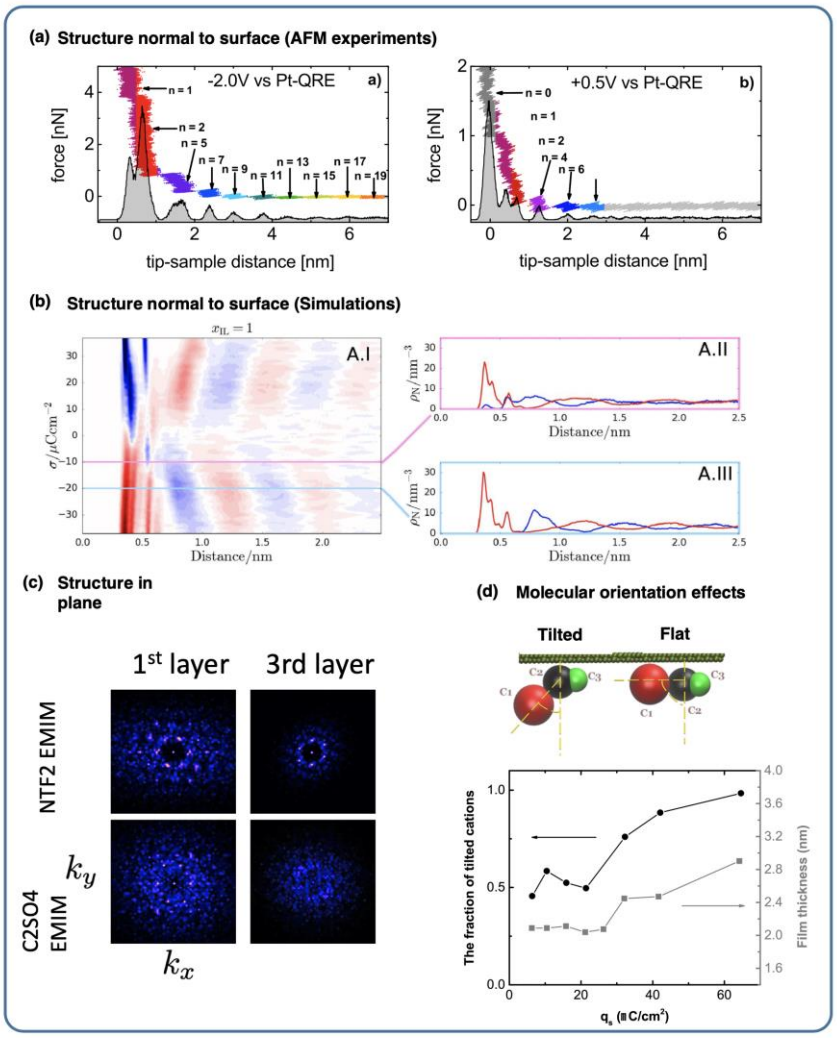

Fig. 2. Effect of surface polarization on ionic liquid film structure. (**a**) Normal forces as a function of tip-electrode distance recorded in AFM measurements for potentials of −2.0 V (*left panel*) and +0.5 V (*right panel*). The force curves are complemented by histograms indicating the probability to find the tip at a given tip−electrode distance (reprinted with permission from ref. 84, ACS). (**b**) *Left panel*: 2D color map calculated for [C4C1Pyrr][NTf2], presenting local difference in number density between cations and anions as a function of distance from a surface and of surface charge density. This map shows alternating layers, preferably containing anions or cations. *Right panels*: density profiles of cation, and anion as a function of distance from the electrode for surface charge of -10 μC/cm^2 (*top panel*) and -20 μC/cm^2 (*bottom panel*). Image reprinted with permission from ref. 87, RCS. (**c**) *Left panel*: Two-dimensional structure factor of the anion rich layer in contact with the charged substrate and the anion rich layer in the interior of the film calculated for the plate charge density of +32 μC cm^{-2} and load of 400 MPa. The top panel represents results for 1-ethyl-3-methyl-imidazolium bis(trifluoromethylsulfonyl)imide and the bottom panel for 1-ethyl-3-methyl-imidazolium ethyl sulfate. The bright spots indicate the formation of 2D crystal structures (reproduced with permission from ref.88, ACS). (**d**) (*Top panel*) "Flat" and "tilted" cation configurations at surfaces with charge density of -32 μC cm^{-2}. (*Bottom panel*) The effect of surface charge density on the relative population of these two configurations (black curve). The ion reorientation induces the swelling of the confined film (grey curve) (reprinted with permission from ref.78, ACS).

MSs have unraveled the microscopic mechanism of EF in RTIL films (see Fig.3) [62,78,77]. The friction force varies with the surface charge density through i) its impact on the normal and in-plane

ordering of the RTIL film and ii) switching between anion and cation layers in contact with substrate surfaces. The charge overscreening, found in RTILs at low and moderate surface charge densities[33], leads to a strong attraction between ionic layers, which slide at the same speed, following a "plug" like profile, with the slippage plane located at the plate-RTIL interface. The friction force increases with the surface charge due to an increase in the sliding energy barriers at the solid-liquid interface. Further increase of surface charge leads to enhanced electrosorption of counterions, resulting in sticking of ionic layers to the solid surfaces and the shift of slippage plane from the plate-RTIL interface to the interior of the film, with the nanofilm featuring a Couette type profile. After that point, the friction starts to go down with further charging. Thus, the friction force exhibits a maximum (see Fig. 3a), which signals the Plug-Couette flow dynamic transition. Such electric-field-induced shift of the slippage plane from the solid−liquid interface to the interior of the film has been observed both in CG and fully atomistic models[62, 88] – in crystalline and disordered nanofilms, and smooth and rough substrates[89] . These findings support the generality of the discussed dynamic transition (see Fig.3b), which is specific to ionic fluids, as it emerges from strong ionic correlations that enable the motion of the confined liquid at sufficiently high loads as a single unit (plug). At high surface charges, the strong adsorption and reorientation of RTIL ions at the surfaces leads to a break in the symmetry of the structure of the confined liquid, modifying the flow mechanism (Couette) and the position of the slippage plane, which determine the friction force. Recent AFM experiments with RTIL confined between gold surfaces and magnetic tip supports the emergence of maximum friction with increasing surface potential[84] (see Figure 3b).

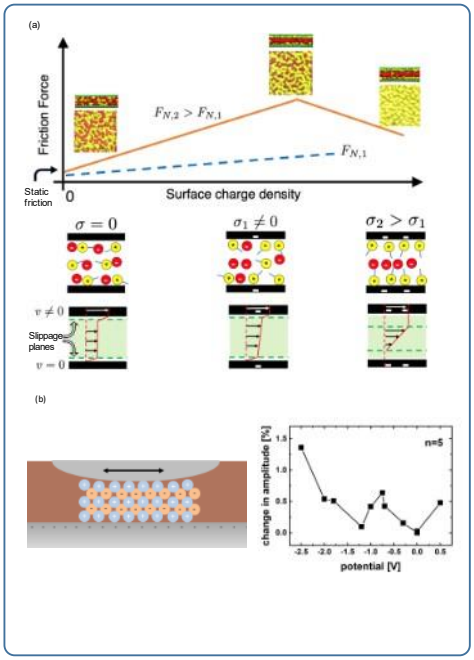

Fig. 3. Mechanism of electrotunable friction in nanoscale RTIL films. (**a**) (*Top panel*) Schematic plot showing the variation of friction force with surface charge density for two different normal loads. At high normal loads, the friction force exhibits a maximum (brown line), whereas for a low load (blue dashed line) a maximum in friction force is shifted to very high surface charges. The insets show snapshots of the confined film structure, obtained for zero, low and high surface charge densities using NEMD simulations of BMIM BF_4. Red, yellow, and green spheres represent the anions, cations, and substrate atoms, respectively. (*Middle panels*) Reorganization of the confined RTIL with surface charging showing an alternating charge density in the perpendicular direction to the substrate plane. Further plate charging leads to accumulation of counterions (cations in the schematic) at the substrate overcompensating the plate charge, while the co-ions (anions) are displaced towards the film interior, (*Bottom panels*) Effect of charging on the flow mechanism of RTIL nanofilms. At low surface charges and high load, the whole film exhibits a Plug-like velocity profile (red line in left panel), while at high surface charges the counterions are strongly adsorbed at the surfaces and the film features Couette flow (right panel). The Plug-Couette dynamic transition gives rise to a friction force maximum, and it is connected to the shift of the slippage plane (green dashed lines in the panels) from the substrate-RTIL interface to the film interior. (**b**) *(Left panel)* Schematics of experimental setup for measuring dynamic shear properties of nanometer-confined RTILs, where the AFM tip oscillates laterally with nanometer scale amplitudes. *(Right panel)* Potential dependence of frictional energy dissipation for five confined layers, supporting the emergence of maximum friction with increasing surface potential shown in panel (a). (image reprinted from ref.84 with permission, ACS).

The RTIL's chemical composition and the polarity of the surface significantly impact the friction forces (see Fig.4a). RTILs with small cations (EMIM) show a better lubrication performance (lower friction forces and higher resistance to squeeze out) than cations with long hydrocarbon chains[77]. Low friction forces were reported for RTILs confined between positively charged surfaces.

Nevertheless, the effect depends on the nature of the anion, and films containing C_2SO_4- anions result in friction forces 60% higher than BF_4- and NTF_2- RTILs[88]. These differences emerge from the lateral ordering induced by the confining surfaces on RTIL nanofilms, with 'crystallization' of the RTIL in the nanogap triggering the effect earlier discovered in structural superlubricity[13], where the enhanced lubrication arises from lattice misfit between the substrate and the RTIL crystal (see Fig.2c). Notably, experimental studies using AFM probes[41] reported a decrease in friction with increasing chain length. This was observed, however, when the tip and electrode were separated by a monolayer of ions. The situation is different for multilayer films discussed in the simulations, where in-plane ordering of the ionic layers leads to a reduction of the friction force.

A key impediment to the widespread use of RTILs as lubricants is, however, their relatively high cost. Hence, recent studies examined the use of RTILs additives to base oil lubricants and the impact of solvents on EF in mixtures are discussed in Box 3.

Box 3 | The role of solvents.

Most RTILs are hygroscopic and absorb water from humid air. Water can be electrolyzed at small electrode polarization, which may be a persistent side effect in applications if water continues to be re-absorbed from the air. This effect demands careful attention, to avoid deteriorating performance of EF devices. Recent experimental and simulation studies showed that, depending on the nature of the ions and how water molecules interact with them, there may be an excess or depletion of water near charged surfaces[90,91,92]. A more usual situation is a substantial excess of water at the electrified interface; this may substantially affect ion layering in nanofilms[58,93,60]. Water appears to increase friction by screening the electrostatic interactions between the ions, modifying the orientation of the ions, the slip conditions at solid-liquid interfaces, and the resistance of the RTIL layers to being squeezed out (see Figs.4 c,d)[60]. The panel below illustrates the structural changes observed in the confined RTIL upon the addition of water. The 'water-dry' ionic liquid is structured in ionic layers of alternating charge. Water molecules adsorb at the charged surfaces and displace the ions from the confined region, thereby disrupting the layered ionic structure. The film thickness (D_1) decreases (D_2) when water is added to the ionic liquid. Notably, presence of even a small amount of water (see blue lines in the right panel) in the film can screen the electrostatic interactions between the ions, making the film more "fluid" and compressible and hence less resistant to external stress. For the same normal load, the film becomes thinner, and the friction increases.

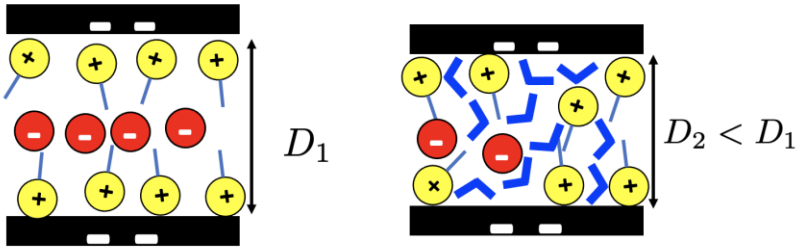

All-in-all, water can be ‘poisonous’ for RTIL lubricants. Experimental studies of BMIM FAP adsorbed at silica surfaces have, however, reported a reduction of friction with increasing water content. This effect may be connected to changes in the silica surface upon water adsorption[94]. In the likely scenario when water can never be fully expunged, ionic liquids need to be ‘designed’ to sustain water, perhaps involving RTIL ions which ligate strongly to water[92]; an important factor to be kept in mind.

Of course, not all neutral molecules are bad for EF. RTILs usually exhibit high viscosities, which impedes mass flow slowing down the dynamic response, essential for switching technologies. The addition of organic solvents to RTILs might provide a solution, first by reducing the cost of RTIL lubricants, and second by enhancing their dynamic response.[95,96] Similarly, to pure RTILs, the lubricating properties of mixtures of RTILs with organic solvents feature a remarkable variation with the electrode charge density, even at low RTIL concentrations (5-10% in an organic solvent, see Fig.4b)[71,97,98] The accumulation of counterions at charged surfaces confining the diluted RTIL solution is responsible for the observed variation of friction forces with surface charge[71,79]. These ion-rich layers adjacent to the charged surfaces are not squeezed out even under very high normal pressures, protecting surfaces from wear and providing excellent lubrication at high loads. Moreover, with appropriate solvents, the friction forces in diluted mixtures can be lower than those in pure RTILs.

< End of Box 3 >

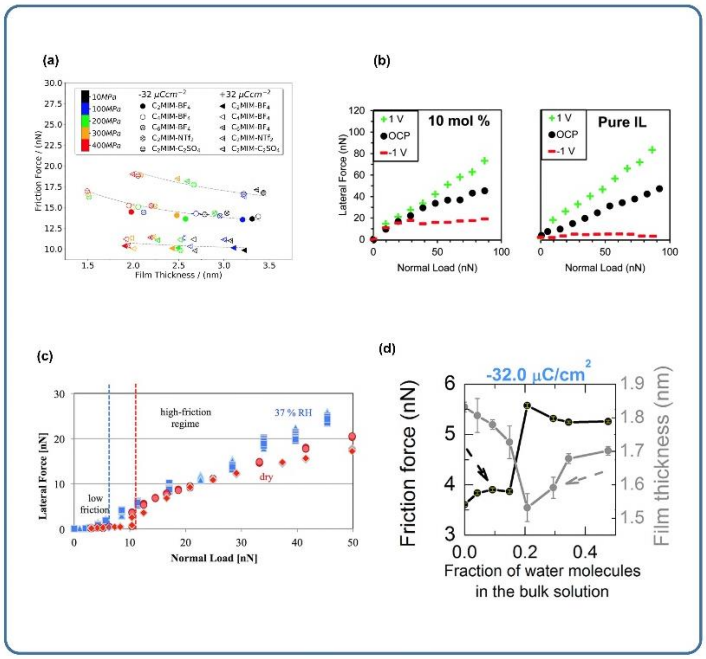

Fig. 4. Effect of film composition on friction (**a**) Dependence of the friction force on the composition of the RTILs and the nanofilm thickness predicted by atomistic simulations[88]. The simulation data cluster in three main groups, which are highlighted by the dashed lines, used here as a guide to the eye. Lower friction forces are observed with EMIM BF_4 or EMIM NTf_2 ionic liquids confined between positively (+32 μC/cm^2, triangles) charged surfaces. Intermediate friction forces are obtained for RTILs confined between negatively (−32 μC/ cm^2 circles) charged surfaces. The highest friction forces shown, correspond to the EMIM C_2SO_4 confined between negatively and positively charged surfaces (image reprinted with permission from ref.88, ACS) (**b**) AFM experiments reveal that tribotronic control of friction, using an external potential applied to a gold surface, is possible for RTIL concentrations as low as 5 mol% in hexadecane. Plot showing the lateral force *vs.* normal load of pure $P_{6,6,6,14}{}^{i}(C_8)2PO_2$ (right) and 10 mol% $P_{6,6,6,14}{}^{i}(C_8)2PO_2$ in hexadecane (left) at different applied potentials (image reprinted with permission from ref.97, RSC). (**c**)-(**d**) Effect of water on friction in nanoscale RTILs. (**c**) Load dependent friction measured with a silica colloidal sphere sliding on mica_in [EMIM][$EtSO_4$] under a dry atmosphere (sphere radius = 9 μm) (red circles and diamonds) and in equilibrated [EMIM][$EtSO_4$] at ambient RH (sphere radius = 7 μm) (blue squares and triangles). The onset of the high-friction regime occurs at a pressure of ∼52 MPa under dry conditions and ∼46 MPa at ambient RH (i.e., under wet conditions) (image reprinted with permission from ref.9358, ACS). (**d**) Friction force and film thickness of BMIM PF6 as a function of bulk water content, computed using NEMD simulations (image reprinted with permission from ref.60, ACS).

Outlook

It is hard to predict, especially the future

(Niels Bohr)

In this article, we overviewed a new field that holds promise for real-time control of friction in mechanical devices. Progress in experimental and simulation studies of friction with RTILs as lubricants showed that using them and applying voltage (i) the friction coefficient can be controlled in real time; (ii) ultra-low friction can be achieved; (iii) strong interactions between the ionic layers

and surfaces can be induced preventing the ‘‘squeeze-out’’ of the liquid and wear under pressure; (iv) robust lubrication performance can be achieved, minimally dependent on changes in the environment due to the low volatility of RTILs. Notably, lubrication by RTILs relies upon two crucial properties which are unusual in their combination: ions are attached strongly to the surfaces through their electrostatic interactions, yet the film retains fluidity under compression. This combination of thermodynamic and kinetic features is one important route to good boundary lubrication and is seen in just a few other scenarios such as in hydration-lubrication[12].

However, fulfilling the promise of EF requires more research. The performance of RTIL lubricants is a complex function of the nature of confining surfaces, their roughness, charge density and polarity, nature of RTIL, temperature and load. While some of these properties are imposed by experimental conditions (e.g. temperature and load) and the specific properties of surfaces (roughness, the surface charge of mineral surfaces), RTILs themselves offer a vast parameter space in terms of their chemical composition, further diversified using solvents and additives. Moreover, electrotunable lubrication relies on controlling surface charges, which can be readily adjusted only on metal or metallized surfaces and coatings. The use of AC fields can open up a new way to tune surface interactions and friction[30,53,54].

While analyzing all these properties implies exploring a huge parameter space, computer simulation studies can help identifying the conditions leading to optimal performance. To achieve electrically controlled lubrication it is necessary to design films where the structure and molecular interactions change significantly in the region where the energy dissipation (slippage) occurs. RTIL nanofilms confined between charged metallic surfaces fulfil this condition.

Encouragingly, and not unexpectedly, the early indications from experiments and simulations, as discussed above, demonstrate that even tiny voltages can yield substantial effects on friction and adhesion between surfaces. Many exciting hypotheses are only now opening to experimental investigation, as new tools have just been made available to incorporate electrodes into high precision surface force and friction experiments[51,99]. Important scenarios and hypotheses yet to be addressed include applying electric fields sufficient to induce 2D phase transitions in nanoscale films and switching from layered to amorphous films by applied potentials**.** While most research is focusing on reducing friction, tribotronic[100] applications might require the opposite, namely finding high friction states by identifying cations-anions pairs leading to friction increase upon switching an external field. This will be useful in smoothening robotic motion, and generally in applications requiring adaptative breaking. Further effects of EF on triboelectricity[101] would also be of interest. For translation of EF to *applications,* it will be necessary to fully characterize the role of surface roughness[89], chemical

degradation of the electrode surfaces resulting from extended cycling, tribochemistry (in particular shear-induced corrosion of RTILs), and all aspects associated to the presence of water, and organic solvent additives. The tree of knowledge in Fig. 5 encapsulates these links.

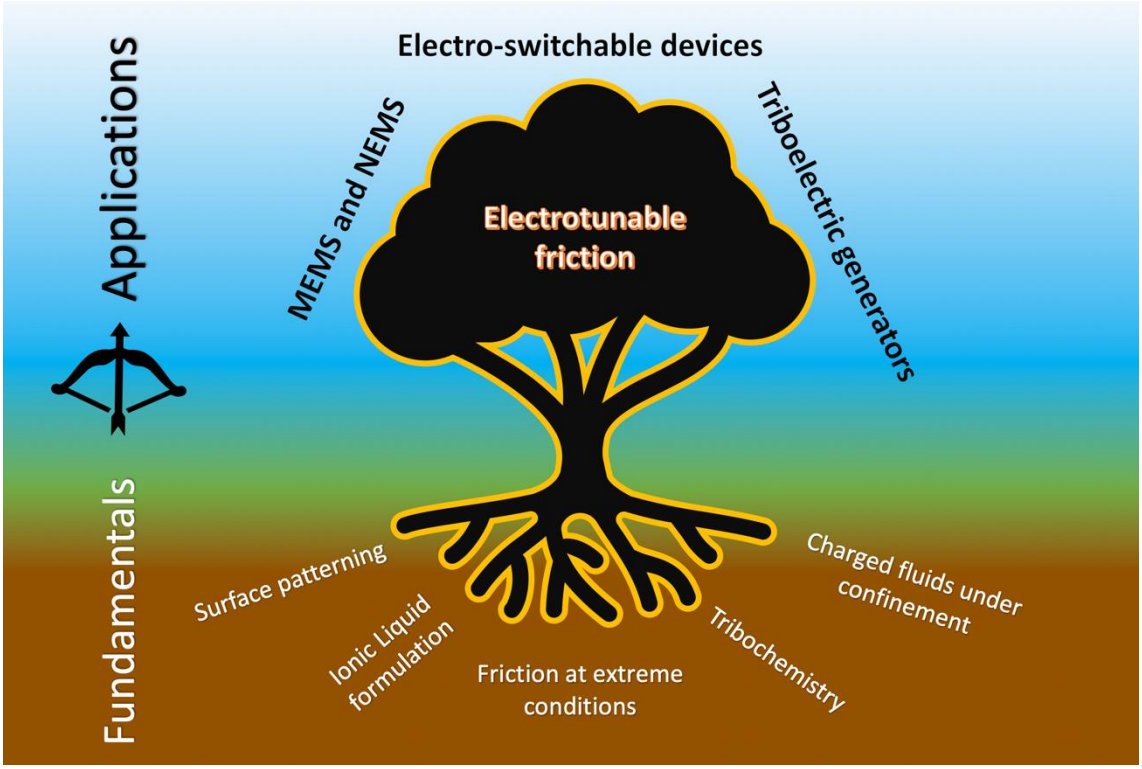

Fig. 5. Electrotunable friction: From fundamentals to applications. Before collecting the fruits in the form of applications – micro/nanoelectromechanical systems (MEMS, NEMS), electro-switchable devices or triboelectric generators, and their deployment possibly in wearable energy conversion devices and robotics, a significant number of explorations need to be performed in the context of the – (i) effect of *surface patterning* of the electrodes on friction, (ii) *formulation* of better ionic liquid lubricants, which goes hand in hand with fabrication of improved surfaces and surface patterning, (iii) *friction and tribochemistry at extreme conditions*, namely high pressure and temperature, which are common for nanocontacts (iv) *tribochemistry*, which opens entirely new scenarios emerging from the interplay of surface interactions, electric fields and chemical reactions, and (v) understanding the properties of *charged fluids under nanoconfinement*, fueled by the importance of nanoconfinement in energy storage. The challenge here will be to develop methods that allow identifying optimum low-cost formulations. Computational methods might help navigate and rapidly screen the library of available RTILs, which virtually contains an endless number of compositions.

When considering applications, we want to be able to control friction, turning it on and off at our will. For instance, in MEM devices or robotics the moving parts should generally move about smoothly, ideally friction-free. But to control their motion we may want to halt that motion abruptly, when needed, but without damaging those parts, or, on the contrary, particularly in robotics, very smoothly, when imitating human motion. This article is a 'manifesto' about how voltage can do this. Will it ever get realized, in the mechanics of movable parts?

One key problem is the avoidance of electrical short cuts. In a capacitor, a dielectric membrane is present separating the two electrodes, which allows ion transport between them, but prevents their mechanical contact. This would be impractical in building electrotunable sliding contacts; instead, at least one of the electrodes must be 'isolated' by dielectric nanoscale solid coating.

Polarizing surfaces of electrotunable device in the same way relative to a reference electrode that is positioned away from the volume where the surfaces move, eliminates the risk of an electrical short circuit. That would, however, present a new challenge of locating suitable reference and counter electrodes and may slow down the friction response to changing voltage.

An optimist may argue, that if we deal with MEMs, where the distances between the rotating plates are mechanically fixed, we can polarize them either way, as those will less likely touch each other. But a tiny deformation can break this down. Therefore, protective insulating layers may be necessary. If, as suggested, we cover one of the surfaces with such layer, voltage will drop across the coating, and so higher voltages may be needed to reach the desired impact on friction. Making the protective layers very thin risks electrical breakdown, so there will always be a trade-off between the value of voltage and the thickness of the protective layers. One could still tolerate in large devices up to 12 V, and, perhaps up to 6V in MEMS.

Detailed scenarios for solving these problems lie beyond the scope of this article. Mechanical and electrical engineers will find together the way to use the described effects, but before that happens, there is still a lot of work for physicists and chemists to do, to find the best ionic liquid lubricants and, perhaps, their mixtures with organic solvents, to investigate the effects of oscillating voltage, of surface roughness, … etc. We hope that this article will motivate further work and enable the growth of the EF-tree, which hopefully will deliver the fruits in due time.

Acknowledgements

F.B, A.A.K. and M.U. are grateful to the Leverhulme Trust for the award of research grant RPG-2016-223. M.U. acknowledges the financial support of the Israel Science Foundation, Grant No. 1141/18 and the binational program of the National Science Foundation of China and Israel Science Foundation, Grant No. 3191/19. SP acknowledges support from the European Research Council, grant number 676861.We would further like to thank Prof. Roland Bennewitz for sharing high-resolution version of some of the images presented herein.

Author contributions F.B., A.A.K., S.P. and M.U. conceived the idea of writing this article, devised its general structure, designed the figures, and contributed to the writing.

Competing interests: The authors declare no competing interests.

Bibliography

1 Holmberg, K. & Erdemir, A. Influence of Tribology on Global Energy Consumption, Costs and Emissions. *Friction* **5**, 263–284 (2017).
2 Jost, P. Lubrication (Tribology) - A Report on the Present Position and Industry's Needs. Department of Education and Science. London, UK: H. M. Stationery Office (1966)
3 Amontons, G. De la Resistance Cause'e Dans Les Machines (About Resistance and Force in Machines). *Mem l'Acedemie R A,* 257–282 (1699).
4 Hutchings, I. M. Leonardo da Vinci's Studies of Friction. *Wear*. 360 (Supplement C): 51–66 (2016).
5 Coulomb, C. A. Sur une Application des Regles de Maximis & Minimis a Quelques Problemes de Statique, Relatifs A I'architecture. *Memoires de Mathematique & de Physique*, presentes a I' Academie. Royale des Sciences par divers Savans, & Ius dans ses Assemblees, **7**, 343–382 (1773).
6 Bowden, F. P. & Tabor, D. The Friction and Lubrication of Solids. New York: Oxford Univ. Press, 1950.
7 Urbakh, M., Klafter, J., Gourdon, D. & Israelachvili, J. The Nonlinear Nature of Friction. *Nature*, **430**, 525-528 (2004).
8 Szlufarska, I., Chandross, M. & Carpick, R.W. Recent Advances in Single-Asperity Nanotribology. *J. Phys. D*, **41**, 123001 (2008).
9 Vanossi, A., Manini, N., Urbakh, M., Zaperri, S. & Tosatti E. Modeling Friction: from Nanoscale to Mesoscale. *Rev. Mod. Phys.* **85**, 529-551 (2013).
10 Rapoport, L., Fleischer, N. & Tenne, R. Fullerene-like WS2 Nanoparticles: Superior Lubricants for Harsh Conditions. *Advanced Materials* **15**, 651-655 (2003).
11 Palacio, M. & Bhushan, B. A Review of Ionic Liquids for Green Molecular Lubrication in Nanotechnology. *Tribol. Lett*. **40**, 247–268 (2010).
12 Raviv, U. & Klein, J. Fluidity of Bound Hydration Layers. *Science* **297**, 1540–1543 (2002).
13 Vanossi, A., Bechinger, C. & Urbakh, M. Structural Lubricity in Soft and Hard Matter Systems. *Nature Communications* 11, 1-11 (2020).
14 Rozman, M. G., Urbakh, M. & Klafter, J. Controlling Chaotic Frictional Forces. *Phys. Rev*. E **57**, 7340–7343 (1998).
15 Socoliuc, A., Gnecco, E, Maier, S., Pfeiffer, O., Baratoff, A., Bennewitz, R.& Meyer, E. Atomic-Scale Control of Friction by Actuation of Nanometersized Contacts. *Science* **313**, 207–210 (2006).
16 Sasak, M., Xu, Y. & Goto M., Control of Friction Force by Light Observed by Friction Force Microscopy in a Vacuum. *Applied Physics Express* **10**, 015201 (2017).
17 Spikes, H.A. Triboelectrochemistry: Influence of Applied Electrical Potentials on Friction and Wear of Lubricated Contacts. *Trib. Lett*. **68**, 90 (2020).
18 Krim, J. Controlling friction with external electric or magnetic fields: 25 examples. Frontiers in Mech. Eng. **5**, 22 (2019).
19 Hausen, F., Gosvami, N. N. & Bennewitz, R. Anion Adsorption and Atomic Friction on Au(111). *Electrochim. Acta*. **56**, 10694– 10700 (2011).
20 Sweeney, J., Hausen, F., Hayes, R., Webber, G. B., Endres, F., Rutland, M. W., Bennewitz, R. & Atkin, R. Control of Nanoscale Friction on Gold in Ionic Liquid by a Potential Dependent Ionic Lubricant Layer. *Phys. Rev. Lett.* **109**, 155502 (2012).
21 Li, H., Wood., R.J., Rutland, M.W. & Atkin, R. An Ionic Liquid Lubricant Enables Superlubricity to be "Switched on" in situ Using an Electrical Potential. *Chem. Commun.* **50**, 4368-4370 (2014**).**
22 Strelcov. E., Kumar, R., Bocharova, V., Sumpter, B.G., Tselev, A. & Kalinin, S.V. Nanoscale Lubrication of Ionic Surfaces Controlled via a Strong Electric Field. *Scientific Reports* **5**, 8049 (2015).
23 Krämer G., Hausen F. & Bennewitz R. Dynamic Shear Force Microscopy of Confined Liquids at a Gold Electrode. *Faraday Discuss*. **199**, 299-309 (2017).
24 Israelachvili, J. Intermolecular and Surface Forces. Academic Press, London, 3rd edn, 2011.
25 Perkin, S., Albrecht, T. & Klein, J. Layering and Shear Properties of an Ionic Liquid, 1-Ethyl-3-Methylimidazolium Ethylsulfate, Confined to Nano-Films between Mica Surfaces. *Phys. Chem. Chem. Phys.* **12**, 1243-1247 (2010).
26 Fre´chette, J. & Vanderlick, T.K. Double Layer Forces over Large Potential Ranges as Measured in an Electrochemical Surface Forces Apparatus. *Langmuir* **17**, 7620-7627 (2001).

27 Valtiner, M., Banquy, X., Kristiansen, K., George W. Greene, G. W. & Israelachvili, J. N. The Electrochemical Surface Forces Apparatus: The Effect of Surface Roughness, Electrostatic Surface Potentials, and Anodic Oxide Growth on Interaction Forces, and Friction between Dissimilar Surfaces in Aqueous Solutions. *Langmuir* **28,** 36, 13080–13093 (2012).
28 Britton, J., Cousens, N. E. A., Coles, S. W., van Engers, C. D., Babenko, V., Murdock, A. T., Koós, A., Perkin, S. & Grobert, N. A Graphene Surface Force Balance. *Langmuir* **30** (38), 11485-11492 (2014).
29 Tivony, R. & Klein, J. Modifying Surface Forces through Control of Surface Potentials. *Faraday Discuss*. **199**, 261-277 (2017).
30 Perez Martinez, C.S. & Perkin S. Surface Forces Generated by the Action of Electric Fields across Liquid Films. *Soft Matter* **15**, 4255-4265 (2019).
31 Tivony, R, Yaakov, D.B, Silbert & G., Klein, J. Direct Observation of Confinement-Induced Charge Inversion at a Metal Surface. *Langmuir* **31**, 12845−12849 (2015).
32 Hallett, J. P. & Welton, T. Room-Temperature Ionic Liquids. Solvents for Synthesis and Catalysis. *Chem. Re*v. **111**, 3508–3576 (2011).
33 Fedorov, M. V. & Kornyshev, A. A. Ionic Liquids at Electrified Interfaces. *Chem. Rev*. **114**, 2978−3036 (2014).
34 Hayes, R., Warr, G. G. & Atkin, R. Structure and Nanostructure in Ionic Liquids. *Chem. Rev*. **115**, 6357−6426 (2015).
35 Miami, I, Inada T., Sasaki R., & Nanao H., Tribo-Chemistry of Phosphonium-Derived Ionic Liquids, *Tribology Letters*, **40**, 225-235 (2010).
36 Wang, H., Lu Q., Ye C., Liu W. & Cui, Z., Friction and Wear Behaviors of Ionic Liquid of Alkylimidazolium hexaflurophophates as Lubricants for Steel/Steel Contact, *Wear*, **256**, 44-48 (2004).
37 Somers, A.E., Howlett, P.C., MacFarlane, D.R., & Forsyth, M.S. Review of ionic liquid lubricants. *Lubricants* **1**, 3-21 (2013).
38 Bazant, M. Z., Storey, B. D. & Kornyshev, A. A. Double Layer in Ionic Liquids: Overscreening versus Crowding. *Phys. Rev. Lett*. **106**, 046102 (2011).
39 Smith, A. M., Lovelock, K. R. J., Gosvami, N. N., Welton, T. & Perkin, S. Quantized Friction across Ionic Liquid Thin Films. *Phys. Chem. Chem. Phys*. **15**, 15317-15320 (2013).
40 Comtet, J., Nigués, A., Kaiser, V., Coasne, B., Bocquet, L. & Siria, A. Nanoscale Capillary Freezing of Ionic Liquids Confined between Metallic Interfaces and the Role of Electronic Screening. *Nat. Mater*. **16**, 634-639 (2017).
41 Zhang, Y., Rutland, M.W., Luo, J., Atkin, R. & Li.H. Potential-Dependent Superlubricity of Ionic Liquids on a Graphite Surface. *J. Phys. Chem*. C **125**, 7, 3940–3947 (2021).
42 Hoth, J., Hausen, F., Müser, M.H. & Bennewitz, R. Force Microscopy of layering and Friction in an Ionic Liquid. *J. Phys.: Condens. Matter* **26**, 284110 (2014).
43 Jurado, L. A., Kim, H., Arcifa, A., Rossi, A., Leal, C., Spencer N.D. & Espinosa-Marzal, R.M. Irreversible Structural Change of a Dry Ionic Liquid under Nanoconfinement. *Phys. Chem. Chem. Phys.* **17**, 13613 –13624 (2015).
44 Black, J.M., Zhu, M., Zhang, P., Unocic, R.R., Guo, D., Okatan, M.B, Dai, S., Cummings, P.T. Kalinin, S.V. Feng, G. & Balke, N. Fundamental Aspects of Electric Double Layer Force-Distance Measurements at Liquid-Solid Interfaces Using Atomic Force Microscopy. *Scientific Reports* **6**, 32389 (2016).
45 Ebeling, D., Bradler, S., Roling, B. & Schirmeisen, A. 3-Dimensional Structure of a Prototypical Ionic Liquid−Solid Interface: Ionic Crystal-Like Behavior Induced by Molecule−Substrate Interactions. *J. Phys. Chem*. C **120**, 11947−11955 (2016).
46 Goodwin, Z.A.H., Eikerling, M., Loewen H. & Kornyshev, A.A. Theory of Microstructured Polymer Electrolyte Artificial Muscles. *Smart Mater. Struct*. **27**, 075056 (2018).
47 Kornyshev, A. A., A.R. Kucernak, A.R., Marinescu, M., Monroe, C.W., Sleightholme, A.E.S. & Urbakh, M. Ultra-Low Voltage Electrowetting. *J. Phys.Chem. C* **114**, 14885-14890 (2010).
48 Cai, M., Yu, Q., Liu, W. & Zhou, F. Ionic Liquid Lubricants: When Chemistry Meets Tribology *Chem. Soc. Rev*. **49**, 7753-7818 (2020).
49 Drummond C., Electric-Field-Induced Friction Reduction and Control. *Phys.Rev.Lett*. **109**, 154302 (2012).

50 Tivony, R., Safran, S., Pincus, P., Silbert, G. & Klein, J. Charging Dynamics of an Individual Nanopore. *Nature Communications* ***9***, 4203 (2018).
51 van Engers, C. D., Balabajew, M., Southam, A. & Perkin, S. A 3-Mirror Surface Force Balance for the Investigation of Fluids Confined to Nanoscale Films between Two Ultra-Smooth Polarizable Electrodes. *Review of Scientific Instruments* **89**, 123901 (2018).
52 Black, J. M.,' Walters, D., Labuda, A., Feng, G., Hillesheim, P. C., Dai, S., Cummings, P. T., Kalinin, S. V., Proksch, R. & Balke, N. Bias-Dependent Molecular-Level Structure of Electrical Double Layer in Ionic Liquid on Graphite. *Nano Lett*. **13**, 12, 5954–596 (2013).
53 Richter, Ł. Żuk, P. J., Szymczak, P., Paczesny, J., Bąk, K. M., Szymborski, T., Garstecki, P., Stone, H. A., Hołyst, R. & Drummond, C. Ions in an AC Electric Field: Strong Long-Range Repulsion between Oppositely Charged Surfaces. *Phys. Rev. Lett*. **125**, 056001 (2020).
54 Perez-Martinez, C. S., Groves, T. & Perkin, S. Controlling Adhesion Using AC Electric Fields Across Fluid Films. *J. Phys.: Cond. Matt.* **33**, 31LT02 (2021**).**
55 Watanabe, S., Pilkington, G.A., Oleshkevych, A., Pedraz, P., Radiom, M., Welbourn, R., Glavatskih, S. & W. Rutland, M.W. Interfacial structuring of non-halogenated imidazolium ionic liquids at charged surfaces: effect of alkyl chain length. *Phys.Chem.Chem.Phys.***22**, 8450-8460 (2020).
56 Rollins, J.B., Fitchett, B.D. & Conboy J.C. Structure and Orientation of the Imidazolium Cation at the Room-Temperature Ionic Liquid/SiO_2 Interface Measured by Sum-Frequency Vibrational Spectroscopy, *J. Chem. Phys*. B, **111**, 4990-4999 (2007).
57 Smith, A. M., Parkes, M. A. & Perkin, S. Molecular Friction Mechanisms Across Nanofilms of a Bilayer-forming Ionic Liquid. *J. Phys. Chem. Lett.* **5**, 4032-4037 (2014).
58 Espinosa-Marzal, R. M., Arcifa, A., Rossi, A. & Spencer, N. D. Microslips to "Avalanches" in Confined, Molecular Layers of Ionic Liquids. *J. Phys. Chem. Lett.* **5**, 179−184 (2014).
59 Perez-Martinez, C. & Perkin, S. Interfacial Structure and Boundary Lubrication of a Dicationic Ionic Liquid. *Langmuir* **35**, 15444-15450 (2019).
60 Fajardo, O.Y., Bresme, F., Kornyshev, A.A. & Urbakh, M., Water in Ionic Liquid Lubricants: Friend and Foe. *ACS Nano*, **11**, 6825–6831 (2017).
61 Bresme, F., Lervik, A. & Armstrong, J. Non-equilibrium Molecular Dynamics, Chapter 6, in Experimental Thermodynamics Volume X: Non-Equilibrium Thermodynamics with Applications, D. Bedeaux, S. Kjelstrup, J.V. Sengers eds., IUPAC, p. 105 (2016).
62 Fajardo, O.Y., Bresme, F., Kornyshev A.A. & Urbakh, M. Electrotunable Lubricity with Ionic Liquid Nanoscale Films. *Scientific Reports*, **5**, 7698 (2015).
63 Roy, D. & Maroncelli, M. An Improved Four-site Ionic Liquid Model, *J. Phys. Chem. B* **114**, 39, 12629–12631 (2010).
64 Canova, F. F., Matsubara, H., Mizukami, M., Kurihara, K. & Shluger, A. L. Shear Dynamics of Nanoconfined Ionic Liquids. *Phys. Chem. Chem. Phys.* ***16***, 8247– 8256 (2014).
65 Fajardo, O.Y., Di Lecce, S. & Bresme, F. Molecular Dynamics Simulation of Imidazolium C_nMIM-BF_4 Ionic Liquids Using a Coarse Grained Force-Field. *Phys. Chem. Chem. Phys.* **22**, 1682-1692 (2020).
66 Capozza, R., Vanossi, A., Benassi, A. & Tosatti, E. Squeezout Phenomena and Boundary Layer Formation of a Model Ionic Liquid Under Confinement and Charging. *J. Chem. Phys.* **142**, 064707 (2015).
67 Lopes, J. N. C., Deschamps, J. & H. Pa´dua, A. A. Modeling Ionic Liquids Using a Systematic All-Atom Force Field. *J. Phys. Chem*. B **108**, 2038-2047 (2004).
68 Yan, T., Burnham, C.J., Del Popolo, M. G. & Voth, G. A. Molecular Dynamics Simulation of Ionic Liquids: The Effect of Electronic Polarizability. *J.Phys.Chem* B **108**, 12 (2004).
69 Nalam, P.C., Sheehan, A., Han, M. & Espinosa-Marzal, R. M. Effects of Nanoscale Roughness on the Lubricious Behavior of an Ionic Liquid, *Adv. Mater. Interfaces* **7**, 2000314 (2020).
70 Zhou, H., Rouha, M., Feng, G., Lee, S. S., Docherty, H., Fenter, P., Cummings, P. T., Fulvio, P. F., Dai, S., McDonough, J., Presser, V. & Gogotsi, Y. Nanoscale Perturbations of Room Temperature Ionic Liquid Structure at Charged and Uncharged Interfaces. *ACS Nano*, **6**, 9818-9827 (2012).
71 Pivnic, K., Bresme, F., Kornyshev, A. A. & Urbakh, M. Electrotunable Friction in Diluted Room Temperature Ionic Liquids: Implications for Nanotribology. *ACS Appl. Nano. Mat.* **3**, 10708–10719 (2020).

72 Merlet, C., Péan, C., Rotenberg, B., Madden, P. A., Simon, P. & Salanne, M. Simulating Supercapacitors: Can We Model Electrodes as Constant Charge Surfaces? *J. Phys. Chem. Lett*. **4**, 264−268 (2013).
73 Seidl,· C., Hormann, J. L. · & Pastewka, L. Molecular Simulations of Electrotunable Lubrication: Viscosity and Wall Slip in Aqueous Electrolytes, Trib. Lett. **69**, 22 (2021).
74 Ntim, S. & Sulpizi, M. Role of Image Charges in Ionic Liquid Confined between Metallic Interfaces. *Phys. Chem. Chem. Phys*. **22**, 10786−10791 (2020).
75 Liu, X. Z., Ye, Z., Dong, Y., Egberts, P., Carpick, R.W. & Martini, A. Dynamics of Atomic Stick-Slip Friction Examined with *Rev. Lett*. **114**, 146102 (2015).
76 Ta, H.T.T., Tran, N.V., Tieu, A.K., Zhu, H., Yu, H., & D. Ta, T.D., *Computational Tribochemistry: a review from classical and quantum mechanical studies*, *J. Phys. Chem. C*, **125**, 16875 (2021).
77 Di Lecce, S., Kornyshev, A.A., Urbakh, M. & Bresme, F. Electrotunable Lubrication with Ionic Liquids: the effects of cation chain length and substrate polarity. *ACS Appl. Mater. and Interfaces* **12**, 4105-4113 (2020).
78 Fajardo, O.Y., Bresme, F., Kornyshev A.A. & Urbakh M., Electrotunable Friction with Ionic Liquid Lubricants: How important is the molecular structure of the Ions? *J. Phys. Chem. Lett*. **6**, 3998-4004 (2015).
79 Pivnic, K., Bresme, F., Kornyshev A.A. & Urbakh M. Structural Forces in Mixtures of Ionic Liquids with Organic Solvents. *Langmuir* **35**, 15410-15420 (2019).
80 Yan, Z., Meng, D., Wu, X., Zhang, X., Liu W. & He, K. Two Dimensional Ordering of Ionic Liquids Confined by Layered Silicate Plates via Molecular Dynamics Simulation. *J. Phys Chem* C **119**, 19244-19252 (2015).
81 Begic, S., Jonsson, E., Chen F. & Forsyth, M. Molecular Dynamics Simulations of Pyrrolidinium and Imidazoium Ionic Liquids at Graphene Interfaces. *Phys.Chem.Chem.Phys*. **19**, 30010 (2017).
82 Dasˇic, M., Stankovic I. & Gkagkas, K. Molecular Dynamics Investigation of the Influence of the Shape of the Cation on the Structure and Lubrication Properties of Ionic Liquids, *Phys. Chem. Chem. Phys*. **21**, 4375—4386 (2019).
83 Capozza, R., Benassi, A., Vanossi, A. & Tosatti, E. Electrical Charging Effects on the Sliding Friction of a Model Nano-Confined Ionic Liquid. *J. Chem. Phys*. **143**, 144703 (2015).
84 Kramer, G. & Bennewitz, R. Molecular Rheology of a Nanometer-confined Ionic Liquid. *J. Phys. Chem*. C, **123**, 46, 28284-28290 (2019).
85 Velpula G.et al, Graphene Meets Ionic Liquids: Fermi level Engineering via Electrostatic forces, *ACS Nano* **13**, 3512-3521 (2019).
86 Zhang, F., Fang, C. & Qiao, R. Effects of Water on Mica−Ionic Liquid Interfaces, *J. Phys. Chem*. C **122**, 9035−9045 (2018).
87 Coles, S.W., Smith, A.M., Fedorov, M.V., Hausen. F & Perkin, S. Interfacial structure and structural forces in mixtures of ionic liquid with a polar solvent. *Faraday Discuss*. 206, 427 (2018).
88 Di Lecce, S., Kornyshev, A.A., Urbakh, M. & Bresme, F. Lateral Ordering in Nanoscale Ionic Liquid Films between Charged Surfaces Enhances Lubricity. *ACS Nano* **14**, 13256−13267 (2020).
89 David, A., Fajardo, O. Y., Kornyshev, A. A., Urbakh M. & Bresme, F. Electrotunable Lubricity with Ionic Liquids: The Influence of Nanoscale Roughness, *Faraday Discuss*. **199**, 279 (2017).
90 Feng, G., Jiang, X., Qiao, R. & Kornyshev, A. A. Water in Ionic Liquids at Electrified Interfaces: The Anatomy of Electrosorption. *ACS Nano* **8**, 11685–11694 (2014).
91 Bi, S., Wang, R.X., Liu, S., Yan, J.W., Mao, B.W., Kornyshev, A.A. & Feng, Minimizing the Electrosorption of Water From Humid Ionic Liquids on Electrodes. *Nature Comm*. **9**, 5222 (2018).
92 McEldrew, M., Goodwin, Z.A.H., Kornyshev, A.A. & Bazant, M.Z. Theory of the Double Layer in Water –in-Salt Electrolytes, *J .Phys. Chem*. Lett. **9**, 5840-5846 (2018).
93 Espinoza-Marzal, R. M., Arcifa, A., Rossi, A. & Spencer, N. D. Ionic Liquids Confined in Hydrophobic Nanocontacts: Structure and Lubricity in the Presence of Water. *J. Phys. Chem*. C **118**, 6491– 6503 (2014).
94 Lertola, A.C., Wang B. & Li, L. Understanding the Friction of Nanometer-Thick Fluorinated Ionic Liquids. *Ind. Eng. Chem. Res*. **57**, 11681−11685 (2018).
95 Wang, J., Tian, Y., Zhao, Y. & Zhuo, K. A Volumetric and Viscosity Study for the Mixtures of 1-n-butyl-3-Methylimidazolium Tetrafluoroborate Ionic Liquid with Acetonitrile, Dichloromethane, 2-Butanone and n, n-Dimethylformamide. *Green Chem*. **5**, 618−622 (2003).

96 Li, S., Zhang, P., Fulvio, P., Hillesheim, P. C., Feng, G., Dai, S. & Cummings, P. T. Enhanced performance of dicationic ionic liquid electrolytes by organic solvents. *J. Phys.: Condens. Matter* **26**, 284105 (2014).
97 Cooper, P. K., Li, H., Rutland, M. W., Webber G. B. & Atkin, R. Tribotronic Control of Friction in Oil-Based Lubricants with Ionic Liquid Additives. *Phys.Chem.Chem.Phys*. **18**, 23657 (2016).
98 Yang, X., Meng, Y. & Tian, Y. Effect of Imidazolium Ionic Liquid Additives on Lubrication Performance of Propylene Carbonate under Different Electrical Potentials. *Tribol. Lett*. **56**, 161−169 (2014).
99 Balabajew, M., van Engers, C. D., & Perkin, S.. Contact-free calibration of an asymmetric multi-layer interferometer for the surface force balance. *Review of Scientific Instruments* **88**, 123903 (2017).
100 Glavatskhi, S & Hoglund, E, Tribotronics-Towards active tribology, Tribology International, **41**, 934-939 (2008).
101 Pam, S & Zhang, Z., Fundamental theories and basic principles of triboelectric effect: A review, Friction, **7**, 2-17 (2019).